RESEARCH ARTICLE

Geometric Optimization of a Mathematical Model of Radiofrequency Ablation in Hepatic Carcinoma

Kai-Feng Wang[1&], Wei Pan[2&], Fei Wang[2], Gao-Feng Wang[1], Pai Madhava[3], Hong-Ming Pan[1], De-Xing Kong[2*], Xiang-Guan Liu[2*]

Abstract

Radio frequency ablation (RFA) is an effective means of achieving local control of liver cancer. It is a particularly suitable mode of therapy for small and favorably located tumors. However, local progression rates are substantially higher for large tumors (>3.0 cm). In the current study, we report on a mathematical model based on geometric optimization to treat large liver tumors. A database of mathematical models relevant to the configuration of liver cancer was also established. The specific placement of electrodes and the frequency of ablation were also optimized. In addition, three types of liver cancer lesion were simulated by computer guidance incorporating mathematical models. This approach can be expected to provide a more effective and rationale mechanism for employing RFA in the therapy of hepatic carcinoma.

Keywords: Radio frequency ablation - mathematical model - geometric optimization - hepatic carcinoma - cover sphere

Asian Pac J Cancer Prev, **14 (10)**, 6151-6158

Introduction

Hepatic carcinoma is one of the most common solid cancers with an estimated annual incidence of at least one million new patients. The incidence of this cancer is especially high in Eastern Asian countries, and it is associated with both higher morbidity and mortality. Radio frequency ablation (RFA) has emerged as the most widely accepted and important method for both early stage and single HCC. It has previously been shown that an effective ablation rate of 98% has been achieved with RFA (Curley et al., 1999). With improvements in treatment devices and techniques, complete necrosis was achieved rates of 70-90% with RFA for HCC ≤5.0 cm in diameter (Livraghi et al., 1999). Additionally, RFA has received significant attention in recent years as a minimally invasive treatment for focal malignant liver disease (Zhou et al., 2010). It should be noted that the main advantage of RFA is the ability of this approach to preserve uninvolved hepatic parenchyma, with destruction of only a small rim of the surrounding healthy liver tissue. Accurate image guidance for optimal placement of the probe into the lesion is of vital importance if complete necrosis of the tumor is to be realized.

One of the drawbacks of RFA, which is related to the size of the tumor, is incomplete tumor ablation. This adversely impacts disease prognosis. A number of studies have estimated that an incompletely ablation to targeted lesion with a diameter greater than 3.0 cm, can subsequently result in high local recurrence after RFA (Solbiati et al., 1997a; 1997b; Kainuma et al., 1999; Livraghi et al., 2000). High local recurrence was found to be related to the size of the RFA area (Cady et al., 1998). Another study reported that under situations where the diameter of the tumor was larger than 5.0 cm, tumor necrosis did not exceed 50% after treatment with RFA, and was thus highly likely to recurrence (Chan et al., 2008).

There have been several studies describing novel methods of establishing mathematical models aimed at enhancing the extent of tumor ablation. Such studies gave way to the realization that an additional surgical margin of 0.5-1.0 cm of apparently normal tissue located adjacent to the tumor, should be preferentially ablated to eliminate the risk of tumor recurrence (Youk et al., 2003; Min et al., 2011).

To reduce relapse rates, an improvement in the efficiency of RFA was needed. For example, Baegert et al. (2007) optimized the trajectory during planning of percutaneous RFA in the liver. In addition, others established a mathematical model based on a geometrically optimized theorem and found that a small change in the precise positioning of the ablated tumor can leave potentially unablated tumor and subsequent treatment failure (Khajanchee et al., 2004). Similarly, Chen et al. used finite-element models in RFA treatment planning, which predicted more physically meaningful therapeutic outcomes (Chen et al., 2009), and one other study developed a modified US-volume system to evaluate

*[1]Department of Oncology, Sir Run Run Shaw Hospital, Medical School, [2]Department of Mathematics, Zhejiang University, Hangzhou, China, [3]HPB Surgical Unit, Department of Surgery and Cancer, Imperial College Healthcare NHS Trust, Hammersmith Hospital campus. London, United Kingdom [&]Equal contributors *For correspondence: dexingkong@126.com, xiangguanliu@yeah.net*

its efficacy in demonstrating a meaningful response to therapeutic RFA (Hiraoka et al., 2010).

The studies discussed above have enabled progress to be made in the field of RFA. However, the methods often lead to a more times of RFA punctures where such approaches often lack practical and effective optimization. Moreover, clinical practice was slow to accept the research and RFA suffered difficulties in popularizing its application since prior studies had not provided an effective way of treating irregular tumors with RFA. Thus, in this report, we have established a mathematical model with a three-dimension database that utilized geometric optimization of RFA. It contains 5 steps to perform including CT scan of liver, three dimension reconstruction of tumor, medical report if tumor, mathematical model established and optimize of RFA by mathematical model. Using this approach, large tumors with diameters greater than 3.0 cm can be targeted effectively.

This study thus focuses on the optimization of RFA in hepatic carcinoma. This approach was based on three model libraries and one untreated model library. These included the pattern of tumors needing corresponding punctures, such as the diameter of the cancer, the maximum section that is perpendicular to the diameter of the tumor and the coordinates of the punctures. In the decision making process, data that characterized the specific tumor were collected, analyzed by a computer software tool, and the frequency and placement of the punctures were decided on by computer simulation.

Materials and Methods

Mathematical model

A geometric optimizing problem was extracted from the optimization of RFA.

Question 2.1. (The cover problem): What are the required and sufficient conditions for an arbitrary N-dimensional graphic (Ω) that can be completely covered by three separate 3.0 cm diameter spheres?

Definition 2.1.1: Graphic (Ω) in N-dimensional space can be covered completely by the graphic if and only if $\forall x \varepsilon \Omega$, then $x \varepsilon H$.

Definition 2.1.2. The diameter (d) in (Ω) of N-dimensional space is defined by $d=max\{d(x_1,x_2) | x_1,x_2 \varepsilon \Omega\}$, where $d(x_1,x_2)$ is the Euclidean distance between x_1 and x_2.

There are four model databases that include 1, 2 and 3-needle databases and an untreatable database. Characteristic data of the tumor patterns are stored in those databases, which need the smallest number of puncture for treatment of the tumors or alternatively, they belong to an untreatable database. If the characteristic data sets of a liver lesion meet the criteria of a database, this lesion will need a corresponding number of punctures for the treatment of the lesion.

Thus, let U_i be the set of tumors that need i needles to treat (i=1, 2, 3) and U_o be the set that need more than three needles to cure. U_j is the set of tumors that need j needles to treat (j=1, 2, 3), the same of U_i. Under these conditions, U is the set of all liver lesions. According to the experimental design of this model, the relationship is established as follows:

$$U_i \subset U_j;\ i<j;\ j=1,2,3$$
$$U_1 \cup U_2 \cup U_3 \cup U_0 \subset U \quad (1)$$

Two dimensional cover model

Current clinical research describes an actual tumor in terms of two-dimensional figures, the major disadvantage of the two-dimensional approach, are first considered as a foundation for the cover problem in 3-dimensional space, thus:

Definition 2.2.1: In R^n (R^n is the n dimension of space. If n=3, that means it is 3 dimensions), $p \varepsilon \Omega$ if and only if there exists a coordinate system and a point $q(q \varepsilon \Omega)$, such that p and q have the same coordinates in this system.

Question 2.2.1: What is the condition that is sufficient for a two dimensional graph Ω, which could be completely covered by three circles with a diameter of 3.0 cm?

Since the maximum area of a graph (it is defined as the area that cover the the longest diameter of the section in two dimension model.) that three separate 3.0 cm diameter circles can cover completely is $6.75\pi\ (cm^2)$, it is assumed that the area (S) of Ω is less than 6.75π, that is $S \leq 6.75\pi$. Two methods are the used to settle this problem, the first approach is referred to as the "inscribed triangle" and the second is referred to as the "subdivision".

Inscribed triangle

In this study, the tumor should be ablated for not more than 3 times of puncture, for it will be more safety and efficacy and with less damage of normal liver tissue. The tips of the RFA needle can be composed into triangle in two dimensions by simulation of the results of CT scan. This method can be transformed into a mathematical problem.

This method is based on the assumption that has an inscribed triangle where the longest edge is less than 3.0 cm. Under conditions where an inscribed triangle in the graph does not meet the assumption, the second mean will be considered. The largest triangle is then selected that satisfies the conditions and draw three separate 3.0 cm diameter circles, centered at the midpoint of each edge (the coordinates of these centers are $[(x', y'), (x'', y''), (x''', y'''),$ respectively]. In addition, because the interior of the triangle is covered completely, one should consider whether the region between the border of Ω and the edges of the triangle are also covered completely. Strictly speaking, if each circle covers a part external to the triangle and is enclosed by its diameter, and Ω's border completely, Ω is considered to be covered completely. Since there are an infinite number of points of a curve, it is impossible to predict whether these points are situated in the interior of one circle. In practice, a finite number of discrete points can be confirmed to ensure that all points are located inside or outside of the interior of the circle, and to enable a mesh subdivision of the curve Ω_1 (Figure 1). The detailed steps involved will be presented in the next method.

Subdivision

The variable Ω is subdivided into mesh with a gap of

α in distance. Then, an appropriate coordinate system is established and the node of the mesh has those defined coordinates. The red region is the sum of all the squares that are covered by Ω and it is an inscribed polygon (referred to as γ) of Ω (Figure 2). If we let S_0 be the difference in area between γ and Ω, then it is easy to derive that $\lim_{\alpha\to 0} S_0=0$.

Question 2.2.1 is now modified to ask whether γ could be covered by three circles completely. Since the diameter of the circle is a constant, the area covered by three circles is uniquely determined by the coordinates of the centers of the circles. Under these circumstances, let the coordinates of the center of the circles be $(x', y'), (x'', y''), (x''', y''')$ and if every point of γ is the interior of one of the three circles, γ will be covered completely.

Let n be the number of squares in γ that are not completely in the interior of the three circles where n is the function of $(x', y'), (x'', y''), (x''', y''')$; note that $n(x', y', x'', y'', x''', y''')$. Thus, now the problem becomes one of non-linear programming: $\min n(x', y', x'', y'', x''', y''')$

$$s.t.\begin{cases} x', x'', x'''\varepsilon(\underset{i=1,\ldots,n}{Min}\{x_n\}-r, \underset{i=1,\ldots,n}{Max}\{x_n\}+r \\ y', y'', y'''\varepsilon(\underset{i=1,\ldots,n}{Min}\{y_n\}-r, \underset{i=1,\ldots,n}{Max}\{y_n\}+r \end{cases} \quad (2)$$

In reality, a smaller α leads to a smaller S_0, and the optimal $(x', y'), (x'', y''), (x''', y''')$ will be a suitable solution for practical purposes. There are several optimization algorithms such as GA, which can be used to solve this non-linear programming problem. This will be discussed in subsequent research reports. In this current report, "Subdivision" will be the primary method.

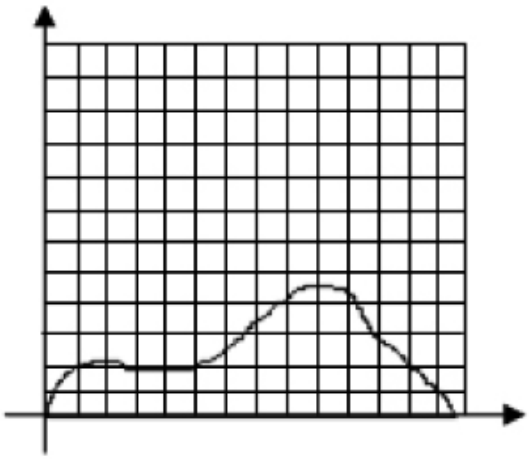

Figure 1. Mesh Subdivision of the Curve Ω_1 in Mathematical Model of Inscribed Triangle

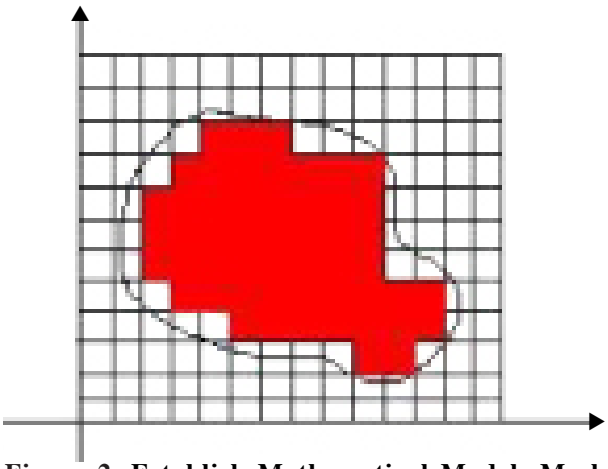

Figure 2. Establish Mathematical Model: Mesh Subdivision of Ω, the Red Area is γ

Model of one ablation

The radius of the sphere is assumed to have a scale r later in the study. Therefore, the area of one sphere can cover a maximum volume of $4\pi r^3/3$. The edges of the cuboids located entirely in one sphere is assumed by the scale a, b and c. Under these circumstances, then a, b and c must satisfy the following inequalities:

$$\begin{cases} a^2+b^2<4r^2 \\ c^2\le 4r^2-(a^2+b^2) \end{cases} \quad (3)$$

Further, when $a^2+b^2+c^2=(4/3)r^2$, the cuboid in the sphere will be the largest, with a volume defined by: volume (v^1_{max}) is $(8\sqrt{3}/9)r^3$.

A necessary yet insufficient condition for one ablation, is that the diameter of the lesion is less than r. It should be noted that a tumor whose diameter is less than r may not be ablated by one ablation. This problem may present itself when shape of the tumor is conical. This conclusion is derived from the following algorithms: *i*) Tumors whose diameter is less than $2r/3$ can be ablated completely by one needle when the center of the ablation sphere is located at the midpoint of the diameter. This is because a cuboid defined as $2r/3\times 4r/3\times 4r/3$ is located entirely in one sphere according to the inequalities defined above, and a tumor whose diameter is less than $2r/3$ is located entirely in this cuboid; *ii*) A tumor whose diameter is r cm in size, belongs to a model library of one ablation, under situation where the center of the ball is at the midpoint of the diameter which completely covers the lesion; and *iii*) For a tumor ranging in size from $2r/3$ cm to r cm, if the center of the tumor is located on the diameter, complete cover of the lesion is equivalent to that of the furthest point from the center in any section, perpendicular to the diameter which is completely covered.

Let the diameter BC be the x-axis, where B is the origin and C is at $(x_1, 0)$. The center of ablation sphere is $A(x_1, 0)$ and r is the radius; thus the longest distance from a point of the section perpendicular to the diameter to the foot $D(x_1, 0)$ is $t(x)$ (Figure 3). Therefore, here the lesion is ablated completely if and only if

$$t^2(x)+(x+x_0)^2\le r^2, \forall x\varepsilon(0, x_1) \quad (4)$$

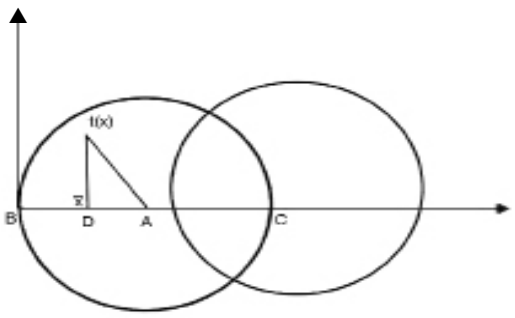

Figure 3. One Ablation Treatment of Tumor in Mathematical Model Establishing

Model of two ablations

It is apparent that the area which two spheres can maximally cover is $8\pi r^3/3$ in volume, and the area that two spheres cover is calculated thus, when these two spheres intersect: The distance between two centers is assumed with a scale of $d(0<d<2r)$. Then for the area (v^{2d}) two spheres cover, the following equation is established:

$$v^{2d}=(8\pi r^3/3)-2\int_0^{2r-d}(2rx-x^2)\pi dx \\ =(8\pi r^3/3)-\{[2(r+d)(2r-d)^2]/3\}\pi \quad (5)$$

When two spheres intersect, a, b and c (representing edges of the cuboids located entirely in the two spheres) should suffice the following inequalities:

$$\begin{cases} a^2+b^2\le 4r^2-d^2 \\ c\le \sqrt{4r^2-(a^2+b^2)}+d \end{cases} \quad (6)$$

Further, the largest cuboid is calculated as following: Set $\xi=a^2+b^2$, then

$$v^2=abc\le ab(\sqrt{4r^2-(a^2+b^2)}+d) \\ \le(a^2+b^2)/2(\sqrt{4r^2-(a^2+b^2)}+d)=(\xi/2)(\sqrt{4r^2-\xi}+d)=f(\xi)$$

By analyzing the function $f(\xi)$, v^2_{max}, the following equation is given:

$$v^2_{max}=f_{max}=\begin{cases} f(4r^2-d^2),\ (2\sqrt{5}/5)r\le d\le 2r \\ f[(8/9)(2r^2+d^2+\sqrt{4r^4-5r^2d^2+d^4}),\ 0<d<(2\sqrt{5}/5)] \end{cases} \quad (7)$$

Here, v^2_{max} is the largest area of the cuboid located in two spheres.

Let the diameter of the tumor be h and x be the axis on the line of the diameter with the node of the diameter as the origin. Thus, $t(x)$ is the largest length between the point whose x-coordinate is x and the point of $(x, 0)$. An assumption here is that the centers of the ablation spheres are placed on the diameter. The intersection of two ablation spheres is a circle with l (where l is a variable whose independent variable is the coordinates of the centers) in radius (Figure 4).

Let two of the centers coordinates be $(x_1, 0)$, $(x_2, 0)$ respectively and $x_2=max\{x_1, x_2\}$, so that $x_2+r\ge h$. When $0\le x\le h$, if $t(x)$ meets the following two inequalities:

$$\begin{cases} t\le \sqrt{r^2-(x_1-x)^2}, & 0\le x\le x_1+\sqrt{r^2-l^2} \\ t\le \sqrt{r^2-(x_2-x)^2}, & x_1+\sqrt{r^2-l^2}\le x\le h \end{cases} \quad (8)$$

The lesion belongs to the model of which the tumor requires treatment with two ablations, that is to say, under conditions here only two spheres can completely cover the lesion. The centers of two spheres represent the location for the acupuncture point. The Subdivision method is then used to verify a graphic of whether it satisfies equation (8) above. Namely, for a group of points $(x_i, t_i(x_i))$, if all of these points meet the requirements of equation (8) above, then it can be entirely covered.

Model of three ablations

In the first instance, denote the domain of the cancer as Ω. Any three centers are in one plane, so let this plane be the XOY plane and let three center points be A, B, C, and the line of AB be the X axis. Additionally, let A be the origin of XOY, the radius of these three spheres be r, the distance between A and B be e_1; the distance between A and C be e_2; the distance between B and C be e_3 and the angle from the AC line to the X axis be θ. Note that this coordinate system is defined as υ (as indicated in Figure 5).

The largest area that 3 spheres can cover is defined as $4\pi r^3$. Similarly, the area where 3 spheres intersect is calculated according to the following equation:

$$v^{3d}=2(v_a+v_b+v_c+v_d+v_e)$$

$$\begin{cases} v_a=\int_{l_{AB}}^{r}3\pi r_1^2dz \\ v_b=\int_{l_{AC}}^{l_{AB}}\{3\pi r_1^2-[r_1^2\arccos(e_1/2r_1)-e_1\sqrt{r_1^2-(e_1/2)^2}]\}dz \\ v_c=\int_{l_{BC}}^{l_{AC}}\{3\pi r_1^2-[r_1^2\arccos(e_1/2r_1)-e_1\sqrt{r_1^2-(e_1/2)^2}]- \\ \quad [r_1^2\arccos(e_2/2r_1)-e_2\sqrt{r_1^2-(e_2/2)^2}]\}dz \\ v_d=\int_{h}^{l_{BC}}\{3\pi r_1^2-[r_1^2\arccos(e_1/2r_1)-e_1\sqrt{r_1^2-(e_1/2)^2}]- \\ \quad [r_1^2\arccos(e_2/2r_1)-e_2\sqrt{r_1^2-(e_2/2)^2}]- \\ \quad [r_1^2\arccos(e_3/2r_1)-e_3\sqrt{r_1^2-(e_3/2)^2}]\}dz \\ v_e=\int_0^h\{S_{\triangle ABC}+[(e_1/2)\sqrt{r_1^2-(e_1/2)^2}]+[(e_2/2)\sqrt{r_1^2-(e_2/2)^2}]+ \\ \quad [(e_3/2)\sqrt{r_1^2-(e_3/2)^2}]+\pi r_1^2\times[(\theta_1+\theta_2+\theta_3)/2\pi]\}dz \end{cases} \quad (9)$$

where, $0\le e_1\le e_2\le e_3\le 2r$ is supposed, $r_1^2=r^2-z^2$

$l_{AB}=\sqrt{r_1^2-(e_1/2)^2}$, $lAC=\sqrt{r_1^2-(e_2/2)^2}$], $lBC=[(e_3/2)\sqrt{r_1^2-(e_3/2)^2}$

$h=\sqrt{r^2-r'^2}$, r' is the radius of the inscribed circle of $\triangle ABC$.

$\theta_1=2\pi-\arccos(a/2r)-\arccos(b/2r)-\angle A$

$\theta_2=2\pi-\arccos(a/2r)-\arccos(c/2r)-\angle B$

$\theta_3=2\pi-\arccos(b/2r)-\arccos(c/2r)-\angle C$

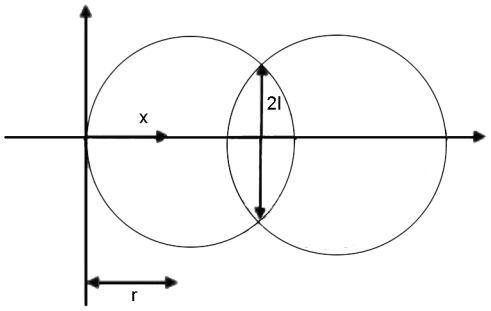

Figure 4. Two Ablations Treatment of Tumor in Mathematical Model Establishing

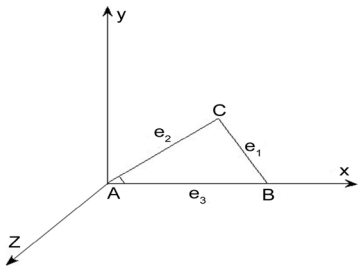

Figure 5. Graphic can be Covered with 3 Spheres. θ: ❑CAB; Distance between A and B: e_1 ; Distance between A and C: e_2; Distance between B and C: e_3

In this equation, e_1, e_2 and e_3 respectively are the scales of three edges of the triangle organized by the centers of the 3 spheres.

When 3 spheres intersect, a, b and c (representing entirely the edges of the cuboids in the 3 spheres) should satisfy the following inequalities:

$$a^2+b^2 \le 4r^2-d^2$$
$$c \le \sqrt{4r^2-(a^2+b^2)}+2d \quad (10)$$

The largest cuboid can thus be calculated following this equation: Set $\xi=a^2+b^2$, then;

$$v_3=abc \le ab[\sqrt{4r^2-(a^2+b^2)}+2d] \quad (11)$$
$$\le [(a^2+b^2)/2][\sqrt{4r^2-(a^2+b^2)}+2d]=(\xi/2)[\sqrt{4r^2-\xi}+2d]@g(\xi)$$

By analyzing the function $g(\xi)$, v^3_{max} is given by:

$$v^3_{max}=g_{max}=g(4r^2-d^2), \quad (2\sqrt{7}/7)r \le d \le 2r$$
$$g(2d^2+2\sqrt{d^4+3r^4-4r^4d^4}), \quad 0<d<(2\sqrt{7}/7)r \quad (12)$$

Here v^3_{max} is the largest area of the cuboid in three spheres. It can be proven that the largest cross-section of the various shapes is composed of three spheres which are located in the XOY plane. In research studies using this model library, the largest section (T) of a patient's lesion is assumed to be placed in the XOY plane.

For any point (x_0, y_0, z_0) of the lesion, if it meets one of the following three inequalities

$$x_0^2+y_0^2+z_0^2 \le r^2$$
$$(x_0-l_1)^2+y_0^2+z_0^2) \le r^2 \quad (13)$$
$$(x_0-l_2\cos\theta)^2+(y_0-l_2\sin\theta)^2+z_0) \le r^2$$

then the tumor can be covered. Thus, under these circumstances, the lesion can be treated when every point of the lesion meets the conditions mentioned above.

Similarly, the subdivision method is used to examine whether one lesion belongs to the model in which a particular tumor can be treated by three needles in an actual test. In order to comply with the strict requirements of a clinical operation, scalar α is set sufficiently small, forming the grid shown in Figure 1. Thus, in Figure 1, each grid is a $\alpha\times\alpha\times\alpha$ cube and its projection on the XOY plane is a $\alpha\times\alpha$ square. For any point $(m\alpha, n\alpha, z_{m,n})$ of the lesion, its projection is $(m\alpha, n\alpha)$. Then, under conditions where the point $(m\alpha, n\alpha, z_{m,n})$ meets one of the inequalities (13), and is equivalent to the lesion, the tumor can be treated by three needles for $\forall m,n,\alpha$ $(m\alpha, n\alpha, z_{m,n})\varepsilon\Omega, \alpha\ge 0, m,n\varepsilon Z$.

The untreatable model

Untreatable lesions refer to those lesions that cannot be treated by three needles. Under this situation, there are three rules that are relevant to the untreatable model: *i*) If the ablation sphere has a radius r, the lesion that has a volume larger than $4\pi r^3$ certainly cannot be treated; *ii*) If the largest section of the lesion has an area(s) larger than $3\pi r^2$ (namely, $S \ge 3\pi r^2$), the lesion also cannot be treated; and *iii*) If a lesion presents with a diameter that is longer than $6r$ (namely $d>6r$), it too cannot be treated

Table 1. The Tumor Parameters of 3 Cases Assessed by Dual Source CT Imaging

Measurement	Patient ID and tumor			
	21****3			21****1
	1	2	3	4
RECIST diameter (mm)	25.8	17.2	42.7	97.9
Max orthog.diameter (mm)	19.2	11	29.2	70.5
z-extension (mm)	30	21	45.5	83
Tumor volume (ml)	5.83	1.92	18.454	283.149
Diameter of volume-equiv.sphere (mm)	22.3	15.4	32.8	81.5

Results

Established an optimized steps of a mathematical model

This study established a optimized mathematical model for RFA in magninant tumor of liver, the procedure is shown as follows: *i*) Reconstruct the three-dimensional (3D) graphic of a tumor lesions according to data obtained from a CT scan; *ii*) Obtain characteristic data of a 3D graphic of the tumor, which should include the diameter, the largest area of the tumor section, etc; *iii*) Compare empirical data with data obtained from the untreatable model library. If these data sets match, this lesion is not treatable (i.e. cannot be treated by three needles). Also, if there is no matching, the lesion will be tested as outlines in step 4 below; *iv*) Sequentially compare the empirical data with data obtained from the model library of one ablation, data obtained from the model library of two ablations and the data obtained from the model library of three ablations so that the optimal treatment scheme can be selected; and *v*) Locate the placement of the electrode according to the model library. If a particular data characteristic of the lesion does not match any model library, the methods proposed in this current report cannot serve to provide optimization proposals. Under this special circumstance, the reader is advised to seek further expert assistance.

The using of optimized mathematical model in liver cancer cases

Three cases, which we will refer to as A (patient ID 21****3), B (patient ID 21****1) and C (patient ID 4****0) were selected to perform simulation by mathematical modeling to establish the above algorithms by a computer software approach. These cases were collected from The Sir RunRun Shaw Hospital and Medical School, Zhejiang University. The parameters of the 3 cases were assessed by Dual Source CT Imaging. The criteria are shown as follows (Table 1).

By the criteria defined above, it was shown that these parameters (i.e., RECIST diameter and Max diameter) were insufficient to determine the specific shape of the lesions. However, we believed it was evident that each lesion was located completely in the cylinder whose height was a RECIST diameter and the radius of the bottom was max orthogonal diameter. This cylindrical approach was used to verify whether it can be covered by three or fewer spheres of which the diameter was 3.0 cm, according to the method described above. If the lesion could be covered, then the lesion was treated. By contrast, if the lesion could not be covered, it was largely uncertain that the lesion could be treated.

*Patient ID: 21****3*

This patient was female, 20 years old. The diagnosis was primary liver cancer, with intrahepatic and lung metastasis, $T_3N_xM_1$, stage IV. This patient came to hospital for abnormal distension and mass. From CT scan it showed that (09/2010): multiple occupying lesions in liver, with port vein embolus and lung metastasis, consider as primary liver cancer. B ultrasound report showed: multiple liver tumors, consider as primary liver cancer. The marker of hepatitis B was positive. This patient was in clinic, treated with Chinese traditional medicine.

Tumor ID: 1

For the cylinder, the diameter of the bottom was 38.4 mm and the height was 25.8 mm: *i*) This lesion did not not belong to the untreatable model library; *ii*) The diameter was approximately 46.2 mm, and did not belong to the model library of one ablation; *iii*) The lesion did belong to the model library of two ablations, because the location on diameter was not searched by the Subdivision approach; and *iv*) The lesion did not belong to the model library of three ablations, because the location in the biggest section of the tumor (rectangle) was not searched by the Subdivision approach. Thus, it was inconclusive whether the cylinder could be covered by three spheres.

Tumor ID: 2

The diameter of the bottom was 22 mm and the height was 17.2 mm: *i*) This lesion did not belong to the untreatable model library; and *ii*) The diameter of the lesion was approximately 27.9 mm. Since the location was searched in the diameter of the lesion, it belonged to a model library of one ablation and the center was placed on the center of the cylinder. Thus, the lesion could be covered by one sphere.

Tumor ID: 3

The diameter of the bottom was 58.4 mm and the height was 42.7 mm: *i*) This lesion did not belong to am untreatable model library; *ii*) The diameter was approximately 72.3 mm (***>2r***), thus it did not belong to a model library of one ablation or a library of two ablations; and *iii*) The lesion did not belong to a model library of three ablations, because the location in the largest section of the tumor (rectangle) was not searched by the Subdivision approach. Thus, it was inconclusive whether the lesion could be covered by three spheres.

In conclusion, it was uncertain whether Tumor ID 1 or Tumor ID 3 were treatable. This was not the case for Tumor ID 2, where it was quite conclusive that this lesion could be treated by one ablation.

*Patient ID: 21****1*

This patient was male, 55 years old. The diagnose of this patient was primary liver cancer with abdominal and bone metastasis, $T_2N_0M_1$, stage IV. This patient came to hospital for the complaint of abdominal and back pain for 3 months. The CT scan showed there was a mass in right liver lobe and peritoneal occupying with bone diseases. The pathology report showed: hepatocellular carcinoma. This patient had taken sorafenib for 1 month. Then he came to hospital again cause of severe abdominal pain.

Tumor ID: 4

The diameter of the bottom was 141 mm and the height was 97.9 mm: *i*) This lesion belonged to the untreatable model library since the diameter was greater than 90 mm (namely, a diameter ***>3r***). Thus this tumor could not be covered by three spheres.

In conclusion: It was inconclusive that Tumor ID 4 was treatable.

*Patient ID: 4****0*

This patient was male, 64 years old. The diagnose of this patient was post operation of primary liver cancer; with recurrence of liver cancer after TACE(transcatheter arterial chemoembolization); liver cirrhosis, $T_2N_0M_0$, stage I. This patient was admitted into hospital for AFP elevated for 9 years and resection of liver cancer for 3 years. The pathology report was hepatocellular carcinoma with liver cirrhosis. The recurrence of liver tumor was found by CT scan (09/2010) after TACE for 3 times.

Tumor ID: 5

The diameter of the bottom was 47.8 mm and the height was 38.3 mm: *i*) This lesion did not belong to the untreatable model library; *ii*) The diameter was approximately 61.2 mm, thus it did not belong to a model library of one ablation or a model library of two ablations; and *iii*) The lesion did not belong to a model library of three ablations, because the location in the largest section of the tumor (a rectangle) was not searched by the Subdivision approach. Thus, this tumor could not be covered by three spheres.

In conclusion, it was inconclusive that Tumor ID 5 was treatable.

Discussion

The target tumor lesion in liver should not exceed 3 cm at its longest axis to achieve best rates of complete ablation using most of the currently available devices according to the expert consensus (Crocetti et al., 2010) and guidelines (Bruix et al., 2001; Bruix and Sherman, 2005). This means the effective ablation range is 3cm (Toshikuni et al., 2010). Although there have already designed many types of RFA needles with the ablation range is up to 7cm, but they were seldom used in clinic because of safety and operators' experience.

A tumor-free margin of less than 1.0 cm was found to be directly associated with an increase in local tumor recurrence (Elias et al., 1998; Poultsides et al., 2010). Similarly, successful RFA of liver tumors depends on inducing coagulation necrosis of the entire tumor and a 1.0 cm thick margin of normal liver located about the 360° perimeter of the tumor (Dodd et al., 2001). In addition, this is also required for multi-direction and multi-angle ablation approaches.

By contrast, conventional 2-dimensional (2D) ultrasound (US) guidance for RFA is limited due to its lower relative sensitivity, in part because of the vapor produced by the high temperatures associated with

RFA when compared with conventional referral modes of therapy such as contrast enhanced computerized tomography (CT) or magnetic resonance imaging (MRI). Also, it is very challenging to accurately position the needle position for the purposes of distinguishing rudimentary tissue from tissue undergoing necrosis during ablation by US. Thus, CT guided RFA exhibits greater reliability, and for liver cancers that are undetectable by US, it is widely considered that CT-guided RFA is effective and relatively safe (Laspas et al., 2009; Park et al., 2009).

In this study, we used CT data acquisition, in which it is straight forward to visualize the 3D spatial aspects of the tumor and its spatial orientation relative to the surrounding hepatic vascular structures. Thus, incomplete ablation and residual lesions may easily occur during RFA, especially for larger liver tumors. Herein, the current study established a mathematical model on the basis of the current radio frequency system to improve the coagulation efficiency and results obtained by RFA.

The overlapping mathematical computing scheme has already been taken considered by other investigators (Rossi et al., 1990; Tsuzuki et al., 1990). Chen et al. established a mathematical model by an ultrasound guided method and used it in clinical trials (Chen et al., 2004). This approach seemed to be more effective than more common conventional approaches. However, for larger tumors, a 14-ablation scheme is considered inoperable in a clinical setting. Thus, a more feasible alternative is to create thermal cylinders, where hyperthermic spheres overlap to create a cylinder. Nonetheless, this model is geometrically less efficient when compared with the 14-ablation scheme, yet, it may still find clinical utility if implemented correctly (Dodd et al., 2000; Rhim et al., 2001). Hence, some investigators proposed that moderate and/or non-infiltrating tumors were treated markedly more successfully more often than larger and/or more infiltrating tumors (Livraghi et al., 2000). We believe it is very important to appreciate the character and tumor growth zone of the lesion being considered for treatment.

In the current study, we analyzed the size of the tumor and infiltration of the tumor by a mathematical modeling approach, and calculated satellite lesions in peritumor, tumor vessels, and the relationship between the tumor and the adjacent organs by this approach. The key objective was to provide the basis for the determination of treatment strategies of RFA.

In conclusion, RFA was found to be more effective than other local ablative therapies (Lau and Lai, 2009). As we know, tumor burden may exceed the ability of current technology to completely ablate the tumor, and thus our ability to affect long-term patient survival is limited (McGhana and Dodd, 2001). Currently, most success of RFA was based on technologic advances in radio frequency electrode and generator design. However, it was clinically useful for the coagulation zone, and induced more complications. Therefore, improvements in the design of methods to ensure adequacy of tumor necrosis is very important.

We theoretically propose clinical research designed to improve the use of RFA in the treatment of large tumors by employing a mathematical model, and features of three-dimensional graphics that can be completely covered by three or fewer spheres. The model provides the mathematical basis for assessing covering problems and its practical effectiveness should be confirmed by computer simulation. In addition, the method of inscribed triangle is an alternative method when studying the coverage problems that are encountered when using three planar circles.

In this study, we have established a mathematical model and a database of hepatic carcinoma for RFA, which we believe can improve the efficiency of RFA. The frequency of accupucture were also optimized, and this approach can also assist the operator design a preferable RFA scheme for patients, in order to reduce the tumor residue. The area of coagulation and configuration of RFA appeared less challenging to predict by calculating the anatomic structure of liver cancer. These results have provided a foundation for an RFA expert system in future studies. In addition, it should be appreciated that the databases derived from the current model are currently insufficient and necessary condition of the actual situation from the design ideas of model base. Once a lesion belongs to a certain model database, it is a sufficient condition but not a necessary condition to require N needles to treat the patient. In other words, if a lesion belongs to a particular model database, then this lesion must be treated by the scheme offered by such database. If a lesion requires N needles for actual treatment, the characteristic data of that tumor may not fit the model base. Therefore, it is our intention to attempt building a complete model database, which will make use of the four model databases to cover all types of tumor lesions, in accord with the following formula: .

Acknowledgements

This study was supported by Medical and Health Platform Backbone Personnel Plan (Department of health of Zhejiang Province, Grant mumber: 2012RCB028); Foundation of China Society of Clinical Oncology (CSCO)-Bayer Schering for young resercher (Grant number:Y-B2010-030).

References

Baegert C, Villard C, Schreck P, Soler L, Gangi A (2007). Trajectory optimization for the planning of percutaneous radiofrequency ablation of hepatic tumors. *Comput Aided Surg*, **12**, 82-90.

Bruix J, Sherman M (2005). Management of hepatocellular carcinoma. *Hepatology*, **42**, 1208-36.

Bruix J, Sherman M, Llovet JM, et al (2001). Clinical management of hepatocellular carcinoma. Conclusions of the Barcelona-2000 EASL conference. European association for the Study of the Liver. *J Hepatol*, **35**, 421-30.

Cady B, Jenkins RL, Steele GD Jr, et al (1998). Surgical margin in hepatic resection for colorectal metastasis: a critical and improvable determinant of outcome. *Ann Surg*, **227**, 566-71.

Chan AC, Poon RT, Ng KK, et al (2008). Changing paradigm in the management of hepatocellular carcinoma improves the survival benefit of early detection by screening. *Ann Surg*, **247**, 666-73.

Chen CC, Miga MI, Galloway RL Jr (2009). Optimizing

electrode placement using finite-element models in radiofrequency ablation treatment planning. *IEEE Trans Biomed Eng*, **56**, 237-45.

Chen MH, Yang W, Yan K, et al (2004). Large liver tumors: protocol for radiofrequency ablation and its clinical application in 110 patients--mathematic model, overlapping mode, and electrode placement process. *Radiology*, **232**, 260-71.

Crocetti L, de Baere T, Lencioni R (2010). Quality improvement guidelines for radiofrequency ablation of liver tumours. *Cardiovasc Intervent Radiol*, **33**, 11-7.

Curley SA, Izzo F, Delrio P, et al (1999). Radiofrequency ablation of unresectable primary and metastatic hepatic malignancies: results in 123 patients. *Ann Surg*, **230**, 1-8.

Dodd GD 3rd, Frank MS, Aribandi M, Chopra S, Chintapalli KN (2001). Radiofrequency thermal ablation: computer analysis of the size of the thermal injury created by overlapping ablations. *AJR Am J Roentgenol*, **177**, 777-82.

Dodd GD 3rd, Soulen MC, Kane RA, et al (2000). Minimally invasive treatment of malignant hepatic tumors: at the threshold of a major breakthrough. *Radiographics*, **20**, 9-27.

Elias D, Cavalcanti A, Sabourin JC, et al (1998). Resection of liver metastases from colorectal cancer: the real impact of the surgical margin. *Eur J Surg Oncol*, **24**, 174-9.

Hiraoka A, Hirooka M, Koizumi Y, et al (2010). Modified technique for determining therapeutic response to radiofrequency ablation therapy for hepatocellular carcinoma using US-volume system. *Oncol Rep*, **23**, 493-7.

Kainuma O, Asano T, Aoyama H, et al (1999). Combined therapy with radiofrequency thermal ablation and intra-arterial infusion chemotherapy for hepatic metastases from colorectal cancer. *Hepatogastroenterol*, **46**, 1071-7.

Khajanchee YS, Streeter D, Swanstrom LL, Hansen PD (2004). A mathematical model for preoperative planning of radiofrequency ablation of hepatic tumors. *Surg Endosc*, **18**, 696-701.

Laspas F, Sotiropoulou E, Mylona S, et al (2009). Computed tomography-guided radiofrequency ablation of hepatocellular carcinoma: treatment efficacy and complications. *J Gastrointestin Liver Dis*, **18**, 323-8.

Lau WY, Lai EC (2009). The current role of radiofrequency ablation in the management of hepatocellular carcinoma: a systematic review. *Ann Surg*, **249**, 20-5.

Livraghi T, Goldberg SN, Lazzaroni S, et al (1999). Small hepatocellular carcinoma: treatment with radio-frequency ablation versus ethanol injection. *Radiology*, **210**, 655-61.

Livraghi T, Goldberg SN, Lazzaroni S, et al (2000). Hepatocellular carcinoma: radio-frequency ablation of medium and large lesions. *Radiol*, **214**, 761-8.

McGhana JP, Dodd GD 3rd (2001). Radiof requency ablation of the liver current status. *AJR Am J Roentgenol*, **176**, 3-16.

Min JH, Lee MW, Rhim H, et al (2011). Recurrent hepatocellular carcinoma after transcatheter arterial chemoembolization: planning sonography forradio frequency ablation. *J Ultrasound Med*, **30**, 617-24.

Park BJ, Byun JH, Jin YH, et al (2009). CT-guided radiofrequency ablation for hepatocellular carcinomas that were undetectable at US: therapeutic effectiveness and safety. *J Vasc Interv Radiol*, **20**, 490-9.

Poultsides GA, Schulick RD, Pawlik TM (2010). Hepatic resection for colorectal metastases: the impact of surgical margin status on outcome. *HPB (Oxford)*, **12**, 43-9.

Rhim H, Goldberg SN, Dodd GD 3rd, et al (2001). Essential techniques for successful radio-frequency thermal ablation of malignant hepatic tumors. *Radiographics*, **21**, 17-35.

Rossi S, Fornari F, Pathies C, Buscarini L (1990). Thermal lesions induced by 480 KHz localized current field in guinea pig and pig liver. *Tumori*, **76**, 54-7.

Solbiati L, Goldberg SN, Ierace T, et al (1997a). Hepatic metastases: percutaneous radio-frequency ablation with cooled-tip electrodes. *Radiology*, **205**, 367-73.

Solbiati L, Ierace T, Goldberg SN, et al (1997b). Percutaneous US-guided radio-frequency tissue ablation of liver metastases: treatment and follow-up in 16 patients. *Radiology*, **202**, 195-203.

Toshikuni N, Takuma Y, Goto T, Yamamoto H (2012). Prognostic factors in hepatitis C patients with a single small hepatocellular carcinoma after radiofrequency ablation. *Hepatogastroenterol*, **59**, 2361-6.

Tsuzuki T, Sugioka A, Ueda M, et al (1990). Hepatic resection for hepatocellular carcinoma. *Surgery*, **107**, 511-20.

Youk JH, Lee JM, Kim CS (2003). Therapeutic response evaluation of malignant hepatic masses treated by interventional procedures with contrast-enhanced agent detection imaging. *J Ultrasound Med*, **22**, 911-20.

Zhou Y, Zhao Y, Li B, et al (2010). Meta-analysis of radiofrequency ablation versus hepatic resection for small hepatocellular carcinoma. *BMC Gastroenterol*, **10**, 78.